J Porous Mater (2017) 24:1581–1593
DOI 10.1007/s10934-017-0398-x

Experimental modelling of copper foams processed through powder metallurgy route using a compressible space holder material

Mohit Sharma[1] · Om Prakash Modi[2,3] · Punit Kumar[1]

Published online: 21 March 2017

Abstract The present work is focused on the processing of open cellular copper foams through space holder technique without the use of binders. In this work, moderate pressures were used during the cold compaction of the powders. The main objective was to obtain dense cell walls by limiting the use of binders and use a compressible and lubricant type of space holder material. It has been shown in this study that the use of high compaction pressure helps to decrease/limit the quantity of binder required and this, in turn, yields relatively dense cell walls necessary for better mechanical strength of foams. Using 2N factorial method, mathematical models have been developed to express the final porosity and pore size as functions of the various processing parameters viz compaction pressure, sintering temperature/ time and space holder content. The most significant sintering parameters influencing the porosity and pore size of the processed foams have also been found out.

Keywords Copper foam · Space holder technique · Acrawax · Powder metallurgy · 2N factorial method

✉ Mohit Sharma
mohit826@gmail.com

[1] Department of Mechanical Engineering, National Institute of Technology, Kurukshetra 136119, Haryana, India

[2] CSIR- Advanced Materials & Processes Research Institute, Bhopal 462064, M.P., India

[3] Department of Material Science & Metallurgical Engineering, Maulana Azad National Institute of Technology, Bhopal, M.P., India

1 Introduction

Owing to the huge potential of being used in a wide variety of engineering applications such as heat transfer, acoustic, orthopaedic applications, porous materials have gained enormous importance these days [1, 2]. In the non-ferrous category, aluminium foams have been extensively researched over the last decade [3–6]. Copper and its composite foams have also gained equal importance due to their potential uses in energy sector as an electrode material for batteries, fuel cells, thermal energy storage, self-lubricated bearings, etc [7–10].

There are numerous ways to process metallic foam out of which methods such as selective laser sintering [11], friction stir processing [12], pressurized casting [13] and powder metallurgical processing [14–20]. Out of these techniques powder metallurgical (P/M) processing of foams has been has been extensively researched in recent years. The biggest drawback of P/M technique, i.e., low density metal matrix, becomes an asset while processing porous materials. One of the P/M techniques of processing foams is the space holder technique [14–20] wherein the pores are dependent on the space holder shape and quantity [21]. The major concern regarding this technique is the stability/intactness of the structure once the space holder gets removed. Several space holder materials have been used by researchers for the processing of foams, for instance, NaCl [16, 17], Sugar [18], Tapioca starch [19], potassium carbonate [14, 15], urea [20–23], magnesium [24]. The use of such a wide range of space holder materials is attributed to the problems associated with each one of them and the urge to find the best possible space holder material. As all the space holder materials have certain advantages as well as disadvantages, it is difficult to make an optimum choice. NaCl has been widely used for

the processing of various elemental foams like titanium and aluminium. However, the removal of salt from the matrix is a time consuming process and the presence of NaCl at sintering temperature leads to chloride impurities in the metal matrix which are corrosive in nature [25]. In view of these drawbacks of using NaCl, table sugar was chosen as an alternative since it is not corrosive. However, the removal of sugar is also quite difficult and time consuming. Jakubowicz et al. [18] compacted titanium powder and sugar at high pressure (500 MPa) so as to keep the metal matrix stable after the removal of sugar by dissolution in hot water. It is worth mentioning here that using such high pressures for a non-compressible/brittle space holder will lead to its fracture and irregular pore formation. Further, for reducing the removal time of space holder, urea was also used as a space holder due to its higher solubility in water. However, it can be inferred here that in some water leachable space holders like NaCl, there are chances that some amount of space holder is always left behind in isolated pores [25]. R. Surace et al. [4] showed that while using salt as the space holder material, some salt always remains behind after the leaching process. However, the NaCl weight fraction (0.06) is much lesser after leaching process and can be neglected.

It becomes important to use a space holder which dissociates or burns off completely due to heat and also the removal is faster. Besides urea, some other materials such as ammonium bicarbonate, tapioca starch, etc were also used for this purpose. The evaporation/dissociation of space holder led to pore formation in the matrix. While this process was fast enough and complete removal was ensured, polluting gases were released during the removal process. Moreover, in this technique, these space holders get removed at low temperature i.e. when the matrix is not strong enough, thereby increasing the probability of collapsed metal structure. Therefore, the use of binder becomes quite essential for the stability of structure after space holder removal. However, the removal of binders such as poly-vinyl alcohol (PVA), silica gel [26], polyethylene [11] is difficult and these materials remain in the metal matrix during the sintering process. Wang et al. [26] studied the effect of binders on the impurity level and sinteribility of foams. It was suggested by the researchers that binders always leave behind some residues on the surface of powders and would thereby affect the sinteribilty. It was also suggested that the reduction of binder content was important keeping in view the mechanical properties of foams. Further, Mu et al. [27] and Schuler et al. [28] discussed the deformation behaviour of the closed and open cellular foams wherein the energy absorbtion/strength of foam is dependent on the gross plastic deformation of the cell walls. This is due to the fact that a poorly sintered or porous cell wall would fracture suddenly and a higher stress concentration on the neighbouring cell walls leads to their cascade failure. It, therefore, becomes important that the cell walls are densified/sintered well in order to ensure good foam characteristics. Further, to increase the strength of cell walls several authors processed composite metal foams [29, 30] which display superior compressive strength compared to their metal counterpart foams.

Another possibility to produce foams with dense cell walls is the lost carbonate sintering method wherein ethanol is used as binder [31]. Ethanol easily evaporates on heating and does not leave behind residues. The space holder material can both be decomposed [14, 15] or leached in water [31]. This process is cost effective and produces foams with good mechanical, electrical and thermal properties [31]. However, it may be pointed out here that the process of sintering is long enough and is performed for 4 h followed by leaching/decomposition time which might increase the overall cost of the process.

In the present work, copper foams have been processed without using binders utilizing slightly higher compaction pressures. Here the emphasis was on selecting a space holder which is compressible and can sustain high compaction pressure without experiencing any fracture. One such promising material chosen in this study is acrawax which is quite commonly as a lubricant during cold compaction. Its chemical name is given as N,N′-ethylene bis-stearamide synthetic wax. The melting point of acrawax is around 140–145 °C and its flash point is 285 °C [32, 33]. It has been shown in earlier studies [34–37] that acrawax decomposes quite easily and leaves no residues. However, as far as the processing of foams is concerned, the use of acrawax as space holder material has received only little attention. Recently, Mondal et al. [34, 35] have used acrawax as the space holder material for processing titanium foams with better mechanical properties and minimum amount of contamination in the metal matrix.

One of the major objectives of the present work is to explore the potential of acrawax as a space holder material and to determine the processing conditions pertaining to best possible results. The other objective is to obtain dense cell walls which are a perquisite for better mechanical properties. Moreover, only few studies [1, 38, 39] have been undertaken to correlate the theoretical and experimental results during the processing of metallic foams. To present the results in a useful form, this paper offers quantitative relationships between the various processing conditions (amount of space holder, compaction pressure, sintering time and sintering temperature) and the final sintered densities and pore size using simple experimental design based upon 2N factorial method. The obtained relationship would be beneficial for obtaining values of final porosity and pore size in the copper foams without undergoing extensive experimentation.

2 Experimental work

Cu powder (average particle size ~ 45 μm and purity 99.5%) supplied by Alfa Aesar, USA and Acrawax (particle size range: 500–1000 micron, 99.5% pure) supplied by Lonza, USA were used as the starting materials (Fig. 1). The Cu powder was mixed with varying quantities of acrawax to obtain two volume fractions −40 and 70%. After uniform mixing, the powder mix was cold compacted using a single action hydraulic press in a 20 mm diameter cylindrical die at two values of applied pressure −200 and 400 MPa. The cold compacted samples were heated at 300 °C for 2 h in a tube furnace with a view to realize complete removal of acrawax which was confirmed through reweighing the compacts after pre-heating. It may be mentioned that the treatment leading to the vaporization of acrawax is termed as pre-heating and samples so treated are called pre-heated samples. The pre-heated powder compacts were then finally sintered in a tube furnace in argon atmosphere for 30 and 60 min at 800 and 900 °C respectively. The heating cycle rate during sintering was kept as 10 °C per min. The pore morphology was examined using a JEOL 5600 scanning electron microscope (SEM) equipped with energy dispersive spectroscopy (EDS) facility. The average pore size in the samples was calculated using ImageJ analysis software from the obtained SEM images of the foams. The final pore shape or size was measured in the direction perpendicular to the loading direction. In elliptical pores, size was measured by measuring the cell in both directions (parallel and perpendicular to loading) and average value was calculated. The density of the sintered samples was calculated with respect to the theoretical density of Cu. The pores obtained through the vaporization of acrawax would be termed as macro-pores and the other pores present in the cell wall regions would be termed as micro-pores in the subsequent text.

Table 1 Parameters upper and lower limits used in the study

Level	Amount of space holder (volume %)	Compaction pressure (MPa)	Sintering time (minutes)	Sintering temperature (°C)
Upper(+)	70	400	60	900
Lower(−)	40	200	30	800
Average	55	300	45	850
Interval	15	100	15	50

The experiments were designed according to the 2N factorial method and the process parameters of interest are sintering time, sintering temperature, compaction pressure and space holder content. Since the number of input parameter'sis four, the numbers of experiments deigned are 16. There were three samples processed for each experiment for checking the repeatability. Table 1 specifies the upper and lower limits of the four process parameters (x_1, x_2, x_3 and x_4) used in this study.This experimental data is fitted into equations for porosity and pore size in the following form [38]:

$$Y = a_0 + a_1X_1 + a_2X_2 + a_3X_3 + a_4X_4 + a_{12}X_1X_2 + a_{13}X_1X_3 + a_{14}X_1X_4 + a_{23}X_2X_3 + a_{24}X_2X_4 + a_{34}X_3X_4 + a_{123}X_1X_2X_3 + a_{124}X_1X_2X_4 + a_{134}X_1X_3X_4 + a_{234}X_2X_3X_4 + a_{1234}X_1X_2X_3X_4 \quad (1)$$

where

$$X_i = \frac{x_i - \frac{(x_i^+ + x_i^-)}{2}}{\frac{(x_i^+ - x_i^-)}{2}} \quad i = 1, 2, 3, 4 \quad (2)$$

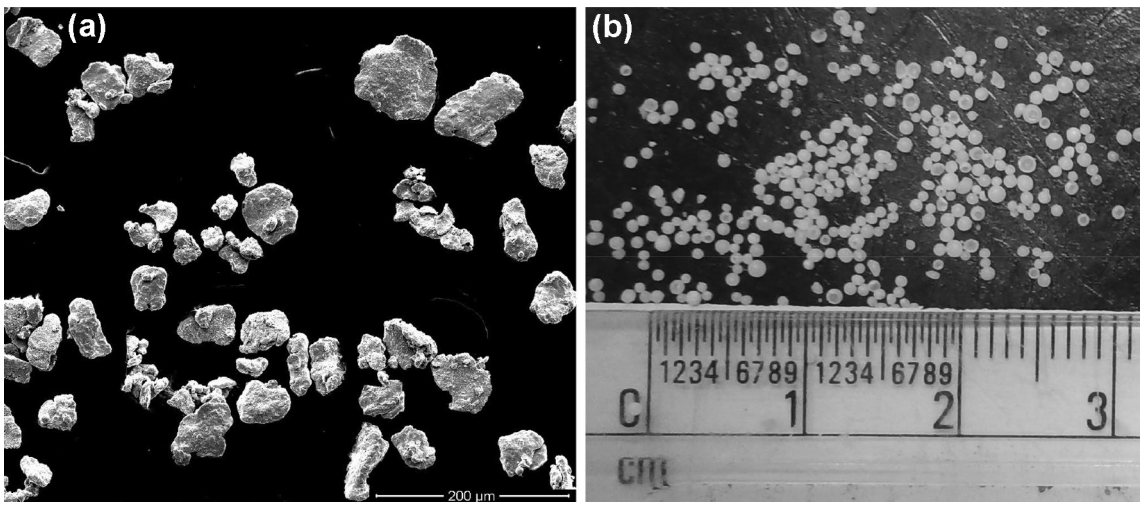

Fig. 1 The morphology of **a** as received Cu powder and **b** as received acrawax beads

3 Results and discussion

3.1 Process parameters

Table 1 shows the parameters used in the study for the experimental modelling. Two values of each process parameter are used in these experiments.The lower and higher values are denoted by '−' and '+' respectively. The content of space holder has been decided according to the final volume porosity desired in the metal matrix.The lower value of porosity was kept as 40 vol% since lower than this value would lead to more number of isolated pores and it would be difficult for the space holder to evaporate out. Eventually, the pressure of the entrapped space holder vapours may lead to cracking and micro-porosity within the cell walls surrounding the pore. The higher value of space holder volume fraction was limited to 70% so that the samples could be successfully processed. It was observed in this study that on increasing the acrawax content to 80 vol%, the sample collapsed after the pre-heating process. This indicates the necessity of a binder for processing samples with space holder content above 70 vol%. Another important observation found was the deposition of the acrawax vapours on the colder surface of the tube present in the alumina tube furnace. It indicates some recovery of the acrawax after the removal of acrawax.

Compaction pressure is another parameter of study and its lower value was taken as 200 MPa as several researchers [14, 15, 25] have compacted metal powders near this value for processing copper foams. The upper limit was set at 400 MPa as a higher compaction pressure leads to excessive deformation of acrawax converting it in form of an ellipse (Fig. 2). Moreover, removal of acrawax in this condition would be extremely difficult since the cell walls around the pore densify at high compaction pressure and the release of vapours would have been very difficult. The values of sintering time have been decided in accordance with the published studies on sintering of powder metallurgical copper samples.The sintering temperature is around (0.8× melting point of material) which comes out to be around 850 °C and therefore, the two values assigned to it are 800 and 900 °C.

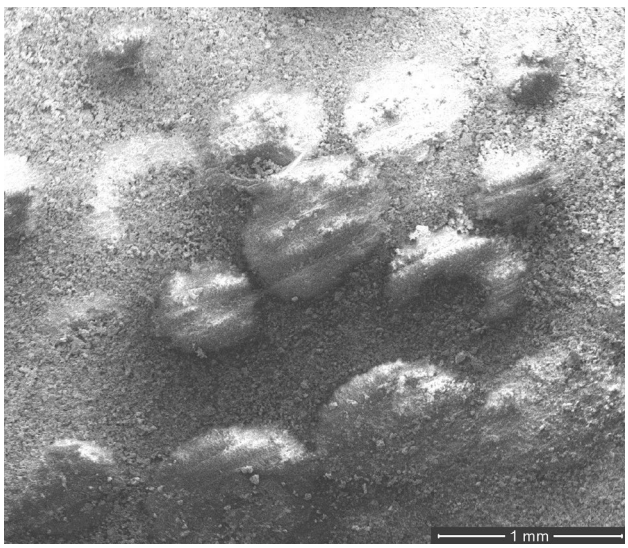

Fig. 2 SEM micrograph of a green compacted sample showing the deformation of acrawax after compacting it at high pressure (>400 MPa)

3.2 SEM study of sintered foams

All the foam samples were prepared successfully and sintered well. However, it was important to closely observe the samples to find out the sintering conditions that yield the best results. Figure 3 shows the optical images of the foams processed under various conditions. On observing (Fig. 3a) 200 MPa compacted samples (40 vol% porosity), they were intact/perfect shaped while high pressure compacted samples (400 MPa, Fig. 3b) with similar porosity had some amount of fragmented sides (marked by arrows). These fragments appear to be formed during the evaporation of acrawax which breaks/weakens the matrix. One of the reasons could be the isolated presence of acrawax in low porosity samples. The matrix was compacted at high pressure reducing the number of channels for acrawax to evaporate off. This in turn led to the breaking of the metal matrix from some sides to facilitate evaporation of acrawax.

On comparing the samples shown in Fig. 3c,d with Fig. 3e,f, the trend reversed. The 70 vol% porous, 400 MPa pressure compacted samples were more intact/perfect shaped compared to 200 MPa samples. This had happened because the samples in this case have more amount of porosity (open pores). During preheating, a larger quantity of acrawax had to evaporate out. High compaction pressure helped in obtaining a stronger metal matrix which sustained the large quantity of acrawax getting evaporated through inter-connected channel of pores. In case of 200 MPa, a weaker matrix could not remain intact due to the evaporating acrawax since there were no binders used. Hence, it can be summarized that when binders are not used, it is advisable to use high compaction pressure for obtaining high porosity foams (>40%) and low compaction pressures for lower porosity foams (<40%).

The foam samples were further characterized using scanning electron microscopy (SEM). Figure 4a shows the samples compacted at 200 MPa and sintered for 30 min at 800 °C. The samples sintered for 30 min exhibit considerable porosity (micro-pores) within the cell wall region (marked by arrows), thereby suggesting that 30 min, 800 °C was not a suitable condition of sintering. On increasing the sintering time to 60 min at 800 °C, the

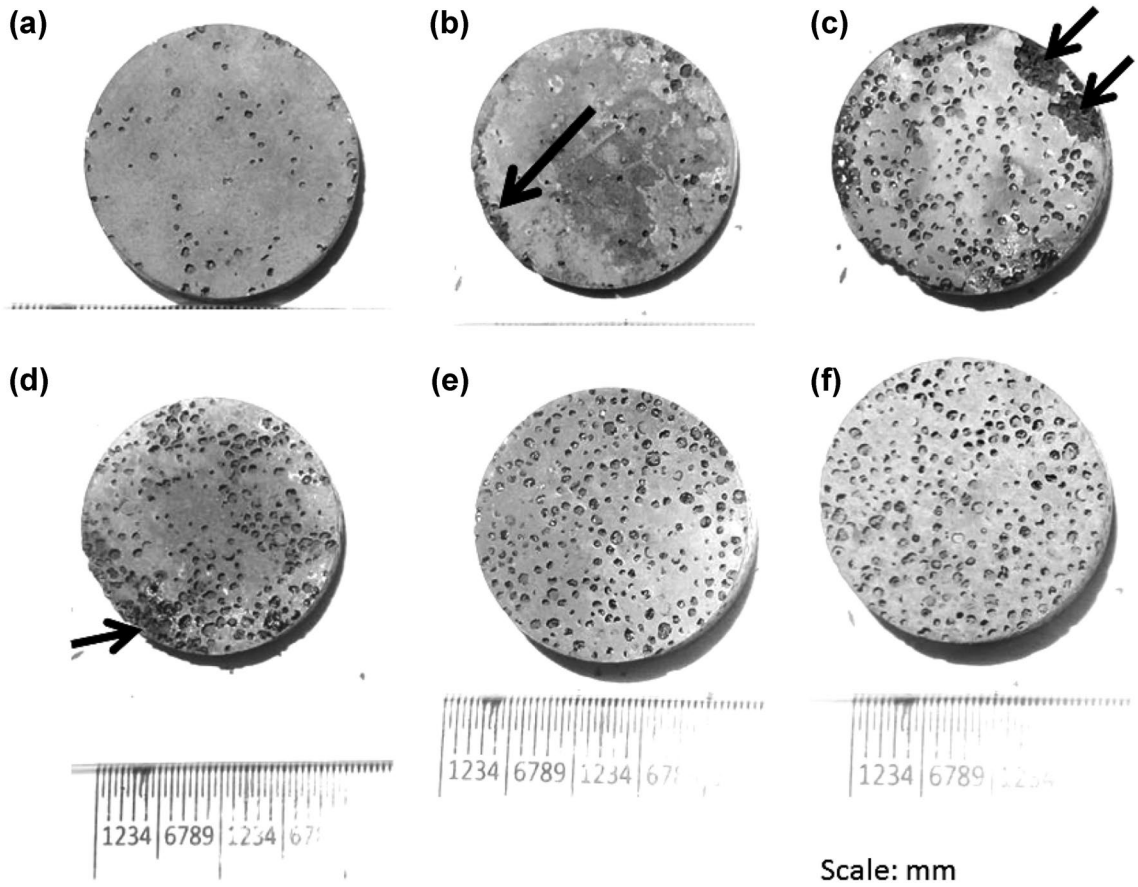

Fig. 3 Optical images of processed foams (vol% porosity-temperature °C-compaction pressure MPa-sintering time min) **a** 40-900-200-60 **b** 40-900-400-60 **c** 70-900-200-30 **d** 70-900-200-60 **e** 70-900-400-30 **f** 70-900-400-60 (*arrows* indicate the imperfection obtained in *shape*)

cell walls became denser (Fig. 4b). The samples contained lesser amount of porosity in the cell wall, suggesting 1 h to be a better choice if sintering is performed at 800 °C.

Figure 5a, b show the samples pertaining to the similar sintering conditions as above, but the cold compaction pressure was used as 400 MPa. The first observation is that the cell walls in this case are denser. Besides, the pores in

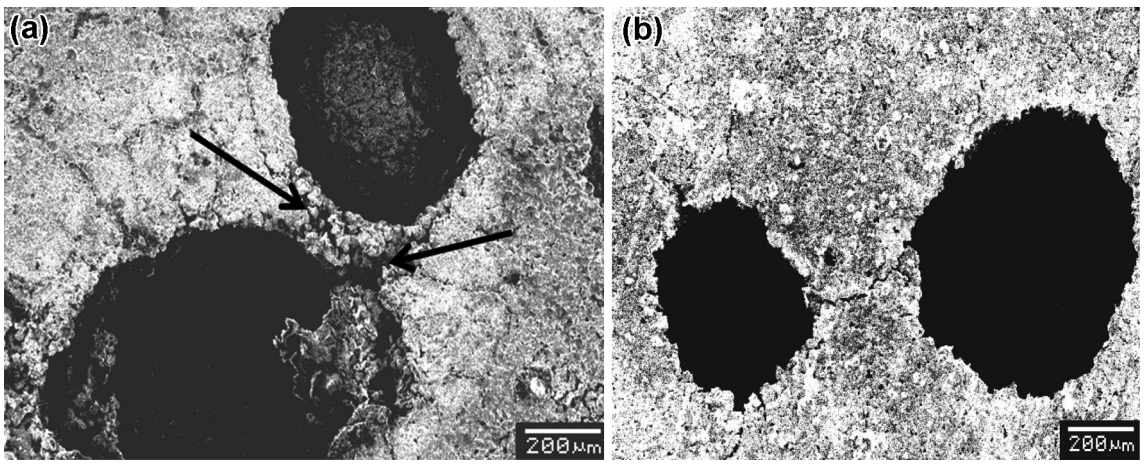

Fig. 4 SEM image of 40% porous samples **a** 200 MPa, 800 °C, 30 min sintered (area represents the porous/unsintered cell wall) and **b** 200 MPa, 800 °C, 60 min sintered showing denser cell walls

the cell walls are much lesser even though sintering was carried out for only 30 min. Here it may be inferred that using high compaction pressure cause the foam samples to be sintered in a shorter duration and/or at lower temperature due to increased metal to metal contact within the cell wall region.

Figure 6a, b show the foam samples sintered at 900 °C for 1 h at 200 MPa and 400 MPa respectively. It is quite obvious that at 900 °C, the samples sintered well and were better than the ones sintered at 800 °C. The cell walls at higher temperature have densified well. However, at 200 MPa (Fig. 6a), the samples still exhibit some amount of micro-porosity in the cell walls while dense cell walls were obtained in 400 MPa compacted samples (Fig. 6b). However, the sphericity of the pores is lesser in the case of using higher compaction pressure. The pores are elongated by certain amount in the loading direction. In Fig. 6b, it can be seen that the pore A is spherical and has smoother internal cell wall surface while the pore B, C, D and E are elliptical and have a wavy surface. The cell wall surface have more of a wavy appearance (shown by white arrows) in the 400 MPa samples compared to 200 MPa compacted samples. This confirms that the space holder material (acrawax) was compressible and the excess pressure led to the deformation of acrawax surface resulting in the wavy nature of the cell wall surface. It can also be observed that the waviness of cell walls increased when the shape of the pore became elliptical. Although, higher pressure has densified the cell wall region more significantly but the sphericity of pores is lesser in 400 MPa samples. The possible difference in the mechanical properties of foams compacted at different pressures can be the subject of future investigations.

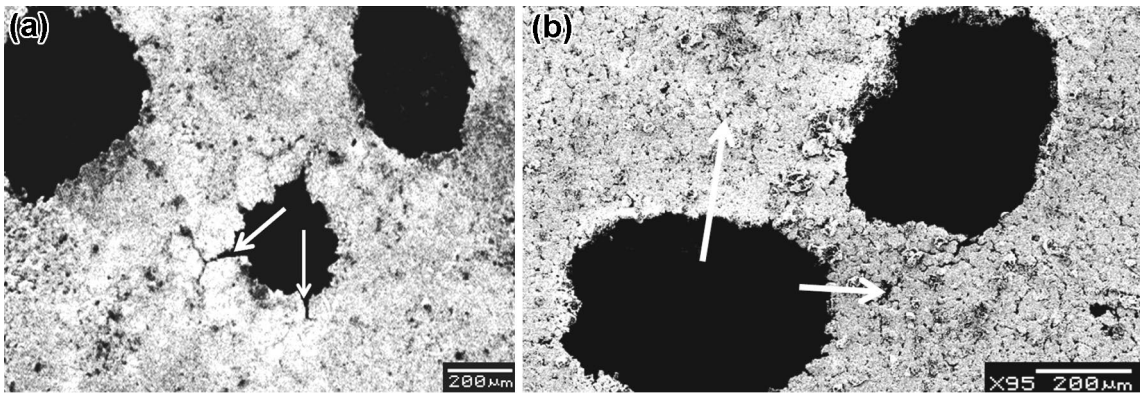

Fig. 5 SEM image of 40% porous samples **a** 400 MPa, 800 °C, 30 min sintered (*arrow* represents the micro-pores in cell walls) and **b** 400 MPa, 800 °C, 60 min sintered showing denser cell walls

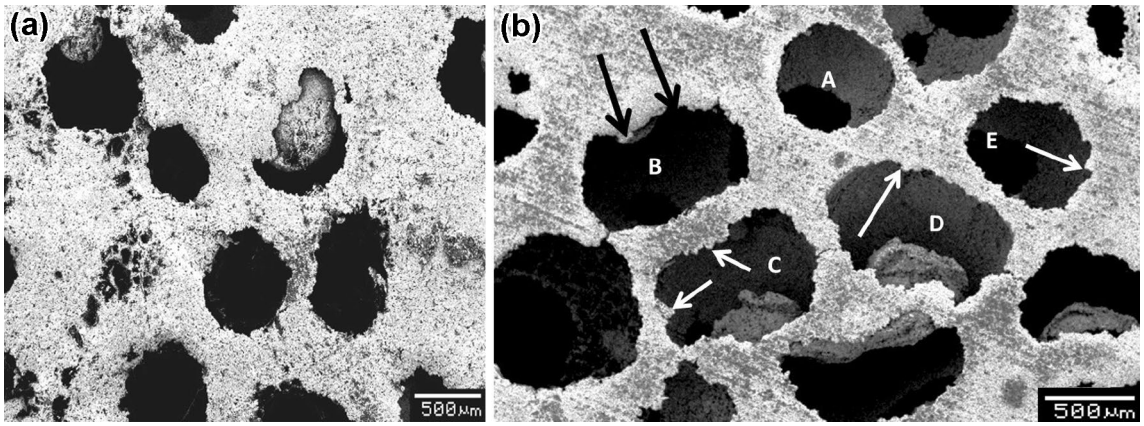

Fig. 6 SEM image of 70% porous samples **a** 200 MPa, 900 °C, 60 min sintered shows micro-pores in cell walls and **b** 400 MPa, 900 °C, 60 min sintered showing denser cell walls (Pore A: circular, Pores B, C, D, E elliptical along loading direction (shown by *black arrows*), metal protrusions (shown by *white arrows*))

However, it has been well stated in earlier studies that the cell walls deform plastically and are responsible for the better energy absorption capacity of foams. Figure 7a, b show magnified images of the cell walls where it becomes obvious that the cell walls are more densified in the case of 400 MPa compared to 200 MPa compacted samples.

3.3 Effect of various processing parameter's on the final sintered density

Figures 8 and 9 shows the porosity plotted with respect to amount of space holder added and compaction pressure. In all the cases, the use of higher compaction pressure produced foams with lower porosity compared to the ones with low compaction pressure. The difference in the porosity in both types of samples (200 and 400 MPa) was much lesser, as can be seen by coinciding data points of porosity (Figs. 8, 9). Table 2 also shows the effect of pressure, sintering temperature/time and space holder content on the final densification achieved. Considering the effect of quantity of space holder, it can be observed that when the acrawax added was 40 vol%, the final sintered density was more than the added volume of acrawax. However, on adding acrawax such that it produced 70 vol% porosity, final sintered density matched with the added amount. The reason behind such difference is that when using a higher volume of acrawax, the pores form more of the interconnected type. This gives easier paths for the acrawax vapours to evaporate out. However, when acrawax content is low, there are not easier paths/ interconnected paths available for the acrawax vapours to get out of the metal matrix. This leads to developing of the outlet paths by the high pressure vapour, leading to some cracks around the pores and an increased micro-porosity within the cell walls which increases the overall porosity above the added quantity of acrawax. The densification rate was faster when the sintering temperature and time were increased [40].

3.4 Effect of various processing parameter's on the final pore size (macro-pores)

Figures 8 and 9 also show pore size plotted with respect to amount of space holder added and compaction pressure. As can be seen, when the space holder content was less (40%), the average pore size was more in 200 MPa and lesser in 400 MPa samples. Considering the samples (40 vol% porosity) sintered at 800 °C, the samples showed no major difference in the pore size after 30 or 60 min of sintering (Table 2). The pore size was marginally smaller when the sintering was carried out for longer duration. Similarly, use of a higher compaction pressure (400 MPa) led to a marginal decrease in the average pore size compared to low pressure (200 MPa) compacted samples.

However, the trend reversed when the samples with 70 vol% porosity were observed. The average pore size in the case of using a higher compaction pressure (400 MPa) was more than the samples processed using lower pressure (200 MPa) in all the experiments. However, the difference in the pore size at 200 and 400 MPa was more in the samples sintered at 900 °C (Comparing the data points in Fig. 8 with Fig. 9). Although, it might appear here that using high pressure should reduce the average pore size but it increased in this case. This difference in the pore size can be explained on the basis of the following points. Using a high pressure would lead to more point to point contacts between the metal powders in the cell wall region. This leads to the faster neck formation/growth and densification of the cell walls. Another point to consider is the pore morphology obtained in both high and low compaction pressures. The pores obtained in low pressure compaction were

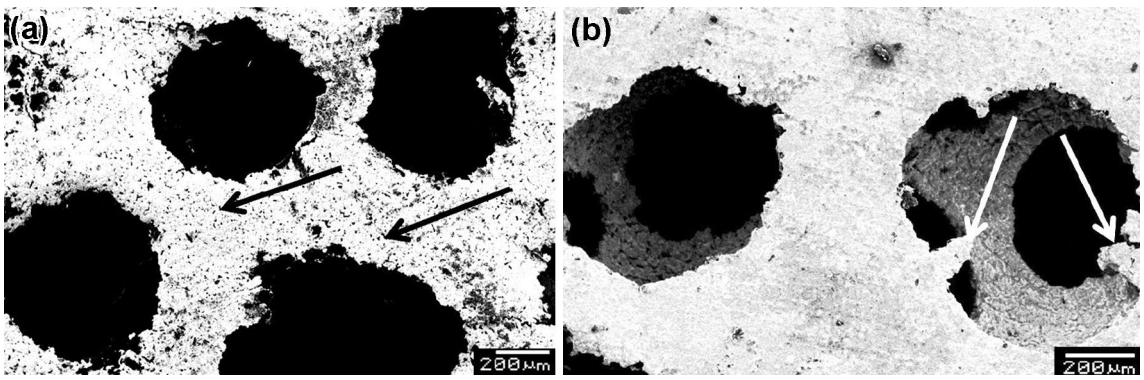

Fig. 7 Magnified SEM image of 70% porous samples **a** 200 MPa, 900 °C, 60 min sintered (*arrow* represents the micro-pores in cell walls) and **b** 400 MPa, 900 °C, 60 min sintered showing denser cell walls (*arrows* show metal protrusions on the inside surface of cell)

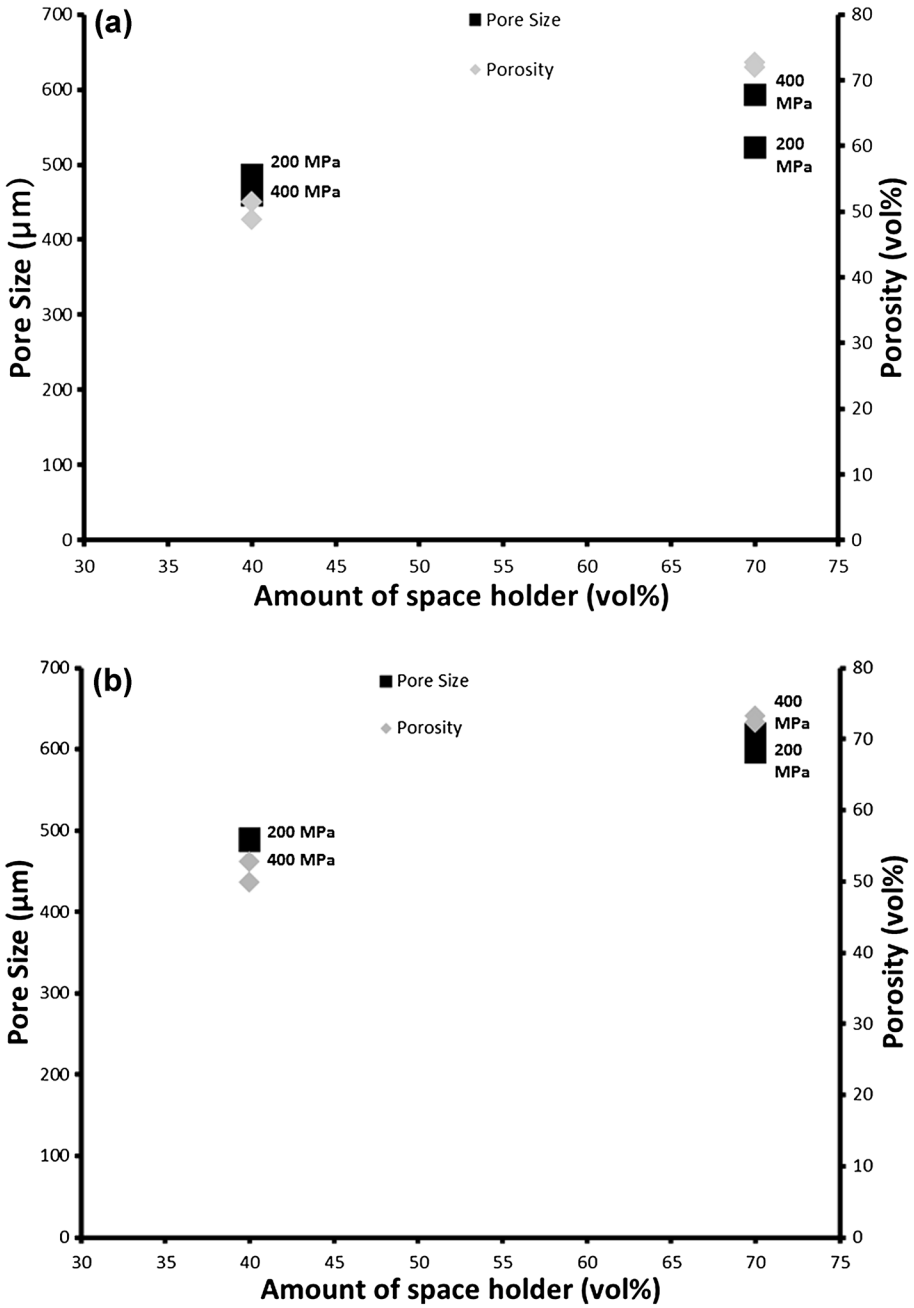

Fig. 8 Effect of space holder and compaction pressure on the porosity and average pore size processed at 800 °C **a** 30 min and **b** 60 min

almost spherical in shape. However, the pores obtained after using higher pressure were both spherical as well as non-spherical (ellipse) in shape. The cell wall region around the elongated pore was in highly stressed condition due to evaporation of acrawax and creation of vapour pressure within the cell. The release of acrawax would have induced a back stress within the cell wall region, causing either some micro-crack to develop around the pores or generate multiple dislocations within the cell wall region. The high dislocation density caused the sintering phenomena to be more dominant in the cell wall regions. Moreover, the regions around the pores have micro-cracks formed during release of acrawax, which would have sintered faster owing to their sharp curvatures and vacancy concentration. These reasons might have led to the densification of the cell walls rather than the shrinkage of pores (macro-pores). As also discussed earlier, all these non-spherical pores had internal surface filled with several metal protrusions (Figs. 6b, 7b). These protrusions show that the metal deposition/transfer has taken place only at some specific positions inside the

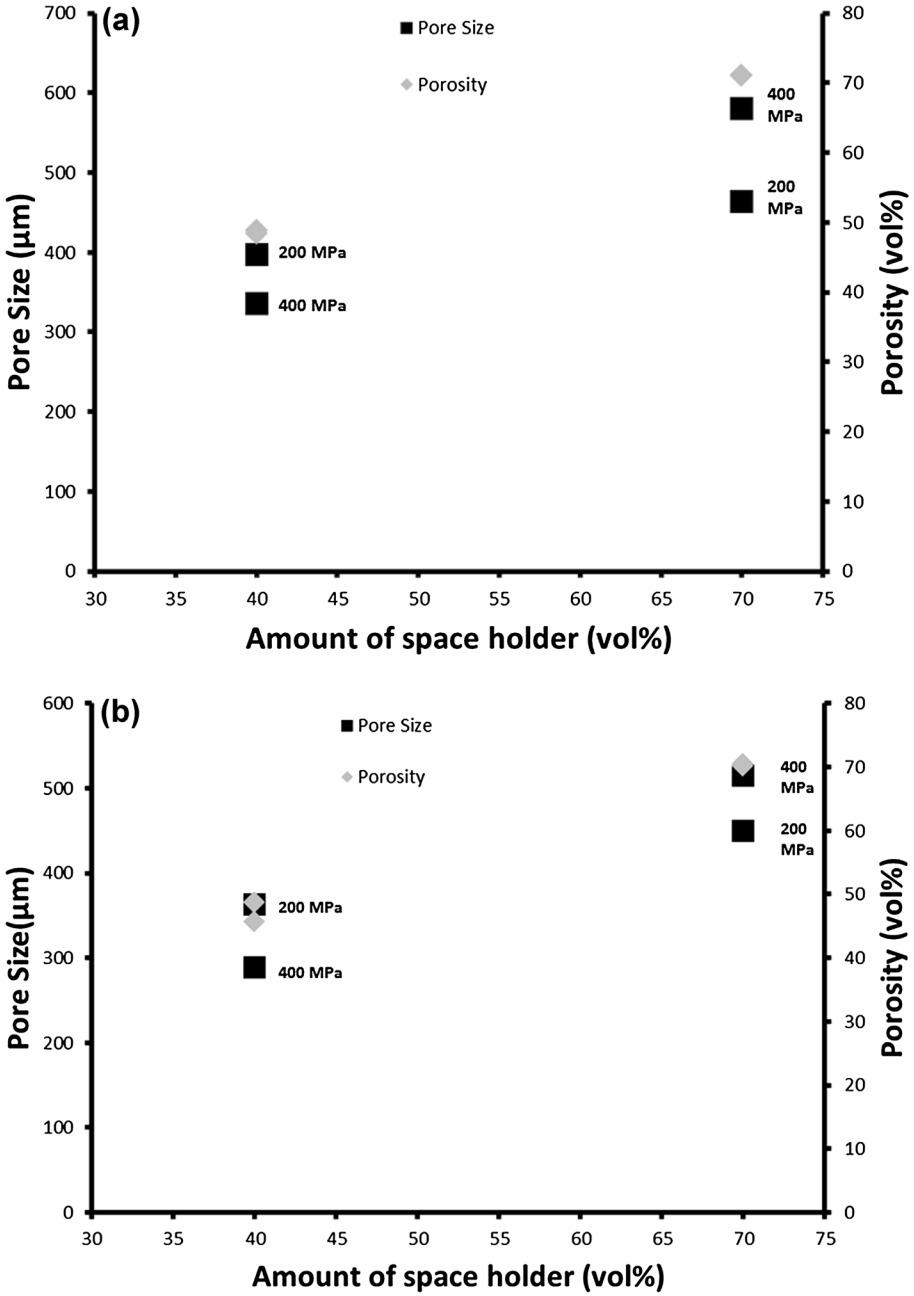

Fig. 9 Effect of space holder and compaction pressure on the porosity and average pore size processed at 900 °C **a** 30 min and **b** 60 min

pore surface rather than the shrinkage of the macro-pore itself. These several points might have influenced the final pore sizes to be larger in case of 400 MPa pressure than the ones obtained in the lower pressure (200 MPa).

At the higher sintering temperature (900 °C), the pore sizes obtained in all the cases were less as compared to the ones obtained at lower sintering temperature (800 °C). This was because the densification is directly proportional to the sintering temperature ($D = Kt^n$: D = densification; K, n = constant; t = sintering temperature [40]). The average pore size in 40 vol% porous samples was lesser when higher compaction pressure was used. Thus, suggesting that high pressure leads to larger pore shrinkage in low porosity samples having more number of the isolated pores.

However, the samples having higher volume % of porosity (70%) showed a similar trend to that of the 800 °C sintered samples. Here also the pores size was more when the higher pressure was used. Therefore, it can be concluded here that high pressure led to more pore shrinkage when the pores were isolated (low porosity samples). On the contrary when the vol% porosity

Table 2 Porosity and pore size data

Exp No.	Volume (%) x_1	Compaction pressure (MPa), x_2	Sintering time (minutes) x_3	Sintering temperature (degree C) x_4	Porosity (%)	Pore size (μm)
1 (433)	40	200	30	800	52.7 ± 0.1	490.6 ± 150
2 (733)	70	200	30	800	73.2 ± 0.2	595.7 ± 170
3 (453)	40	400	30	800	49.9 ± 0.15	487.3 ± 210
4 (753)	70	400	30	800	72.3 ± 0.05	620.2 ± 145
5 (436)	40	200	60	800	51.45 ± 0.2	486.3 ± 135
6 (736)	70	200	60	800	72.6 ± 0.06	523.3 ± 180
7 (456)	40	400	60	800	48.7 ± 0.16	459.1 ± 225
8 (756)	70	400	60	800	71.9 ± 0.23	593.2 ± 155
9 (433)	40	200	30	900	48.8 ± 0.3	396.9 ± 168
10 (733)	70	200	30	900	71.1 ± 0.25	464.5 ± 210
11 (453)	40	400	30	900	48.4 ± 0.14	336.3 ± 174
12 (753)	70	400	30	900	71 ± 0.05	580.2 ± 160
13 (436)	40	200	60	900	48.7 ± 0.3	363.4 ± 170
14 (736)	70	200	60	900	70.5 ± 0.05	450.4 ± 150
15 (456)	40	400	60	900	45.7 ± 0.08	288.8 ± 138
16 (756)	70	400	60	900	70.1 ± 0.04	515.1 ± 160

Table 3 EDS spot analysis at pore periphery in copper foam

Element	Weight %	Atomic %
Copper	4.09	14.47
Oxygen	95.91	85.53

increased (pores become interconnected) high pressure had a reverse effect on the average pore size.

3.5 EDS analysis and comparison with other works carried out

Table 3 shows EDS spot analysis of the processed copper foam. It can be observed from the EDS result that there are no other elemental impurities present. This EDS spectrum showed only copper and oxygen presence throughout the pores and cell wall region. This confirmed that acrawax removed completely from the matrix and left no residues.

Table 4 shows the comparison of various space holder materials used for processing foams. In all of the previous studies there was micro-porosity present within the cell wall region. There has also been lot of difference (~2–4 vol%) in the amount of space holder added and the final porosity achieved after sintering process. In the present study, the foams obtained in EXP 16 (400 MPa) had almost negligible micro-porosity within the cell walls. Also the porosity generated in the EXP 16 condition matched with amount of space holder added. Thereby, suggesting acrawax to be better space holder material which not only resists high compaction pressure but also allows the metal powder to flow around it more efficiently due to its lubricating nature. This helps in producing foams with better

Table 4 Comparison of the micro-pores size and volume obtained in present study with previous studies

Evaporative type space holder material	Micro-porosity (difference with amount of space holder added) (70 vol% porous samples)	Micro-pores size range (micron)	Reference
Carbamide/urea	0.25	10–20	[41]
Ammonium bi-carbonate	2–4	10–30	[42]
Potassium carbonate	5–6	0-200	[43]
Acrawax	10–15	5–12	[35]
Acrawax	0.5 (Exp. 14)	10–20	Present study
	0.1 (Exp. 16)	Negligible	Present study

Table 5 Values of coefficients in Eq. (1)

Coefficients	For porosity	For pore size
a_0	60.4406	478.2063
a_1	11.1469	64.6188
a_2	−0.6906	6.8188
a_3	−0.4844	−18.2563
a_4	−1.1531	−53.7563
a_{12}	0.4281	27.5313
a_{13}	0.1719	−4.0688
a_{14}	0.2406	13.4813
a_{23}	−0.1656	−2.7187
a_{24}	0.2031	−1.1687
a_{34}	−0.0531	−1.7687
a_{123}	0.1531	2.0188
a_{124}	−0.0656	11.9187
a_{134}	−0.0094	4.2938
a_{234}	−0.1969	−5.4063
a_{1234}	0.1344	−6.6438

densified cell walls after the sintering process compared to other space holder materials.

3.6 Mathematical model of final sintered density and average pore size

For obtaining the relationship between the sintering parameter's with the final sintered density and pore size, two equations were solved using MATLAB programming. Here the first matrix [16×4] row in Equations 3 and 4 represents the values of X_1, X_2, X_3 and X_4 for a particular experiment. An example below shows how the values (X_i) were calculated.

Example: Row1,

Exp1 (Table 2) $x_1 = 40\%$; $x_2 = 200$ MPa; $x_3 = 30$ min; $x_4 = 800\,^{\circ}C$.

$X_i = (x_i - \text{average})/\text{interval}$ (average and interval values taken from Table 1).

$X_1 = (40–55)/15 = -1$

$X_2 = (200–300)/100 = -1$

$X_3 = (30–45)/15 = -1$

$X_4 = (800–850)/50 = -1$

Similarly, the X_i values for other experiments were calculated. The second matrix in equations 3 and 4 represents the various coefficient's which are to be obtained (Table 5). The last matrix shows the actual values of final porosity and average pore size obtained after carrying out the 16 experiments (Eqs. 3and 4).

$$\begin{bmatrix} -1 & -1 & -1 & -1 \\ 1 & -1 & -1 & -1 \\ -1 & 1 & -1 & -1 \\ 1 & 1 & -1 & -1 \\ -1 & -1 & 1 & -1 \\ 1 & -1 & 1 & -1 \\ -1 & 1 & 1 & -1 \\ 1 & 1 & 1 & -1 \\ -1 & -1 & -1 & 1 \\ 1 & -1 & -1 & 1 \\ -1 & 1 & -1 & 1 \\ 1 & 1 & -1 & 1 \\ -1 & -1 & 1 & 1 \\ 1 & -1 & 1 & 1 \\ -1 & 1 & 1 & 1 \\ 1 & 1 & 1 & 1 \end{bmatrix} \begin{bmatrix} a0 \\ a1 \\ a2 \\ a3 \\ a4 \\ a12 \\ a13 \\ a14 \\ a23 \\ a24 \\ a34 \\ a123 \\ a124 \\ a134 \\ a234 \\ a1234 \end{bmatrix} = \begin{bmatrix} 52.7 \\ 73.2 \\ 49.9 \\ 72.3 \\ 51.45 \\ 72.6 \\ 48.7 \\ 71.9 \\ 48.8 \\ 71.1 \\ 48.4 \\ 71 \\ 48.7 \\ 70.5 \\ 45.7 \\ 70.1 \end{bmatrix} \quad (3)$$

$$\begin{bmatrix} -1 & -1 & -1 & -1 \\ 1 & -1 & -1 & -1 \\ -1 & 1 & -1 & -1 \\ 1 & 1 & -1 & -1 \\ -1 & -1 & 1 & -1 \\ 1 & -1 & 1 & -1 \\ -1 & 1 & 1 & -1 \\ 1 & 1 & 1 & -1 \\ -1 & -1 & -1 & 1 \\ 1 & -1 & -1 & 1 \\ -1 & 1 & -1 & 1 \\ 1 & 1 & -1 & 1 \\ -1 & -1 & 1 & 1 \\ 1 & -1 & 1 & 1 \\ -1 & 1 & 1 & 1 \\ 1 & 1 & 1 & 1 \end{bmatrix} \begin{bmatrix} a0 \\ a1 \\ a2 \\ a3 \\ a4 \\ a12 \\ a13 \\ a14 \\ a23 \\ a24 \\ a34 \\ a123 \\ a124 \\ a134 \\ a234 \\ a1234 \end{bmatrix} = \begin{bmatrix} 490.6 \\ 595.7 \\ 487.3 \\ 620.2 \\ 486.3 \\ 523.3 \\ 459.1 \\ 593.2 \\ 396.9 \\ 464.5 \\ 336.3 \\ 580.2 \\ 363.4 \\ 450.4 \\ 288.8 \\ 515.1 \end{bmatrix} \quad (4)$$

Equations 5 and 6 represent the obtained mathematical model for final porosity and average pore size. It can be observed from the equations that the final porosity in the samples is more dependent on the amount of space holder compared to any other sintering parameters. However, the average pore size was found to be dependent on both the amount of space holder and the sintering temperatures.

Table 6 Experiments performed to test the validity of equations obtained

S. No.	Volume (%) x_1	Compaction pressure (MPa), x_2	Sintering time (minutes) x_3	Sintering temperature (°C) x_4	Theoretical value	Experimental value	Deviation from theoretical (%)
1	50	400	60	900	53.83, 364.8	54.6, 375	1.4, 2.8
2	30	200	60	900	41.4, 334.8	42.8, 325	3.3, 2.9

Further, for testing the validity of the obtained models, two experiments were performed (Table 6). In the first experiment, the amount of space holder was taken as 50% lying within the data range used to predict the model. In the other experiment, the amount of space holder was chosen as 30%, not lying within the data range. Here it was found in both the cases that the deviation in experimental and theoretical values was approximately 3%.

$$\begin{aligned} Y = {} & 60.4406 + 11.1469X_1 - 0.6906X_2 - 0.4844X_3 \\ & - 1.1531X_4 + 0.4281X_1X_2 + 0.1719X_1X_3 \\ & + 0.2406X_1X_4 - 0.1656X_2X_3 + 0.20131X_2X_4 \\ & - 0.0531X_3X_4 + 0.1531X_1X_2X_3 - 0.0656X_1X_2X_4 \\ & - 0.0094X_1X_3X_4 - 0.1969X_2X_3X_4 \\ & + 0.1344X_1X_2X_3X_4 \end{aligned} \quad (5)$$

$$\begin{aligned} Y = {} & 478.2063 + 64.6188X_1 + 6.8188X_2 - 18.2563X_3 \\ & - 53.7563X_4 + 27.5313X_1X_2 - 4.0688X_1X_3 \\ & + 13.4813X_1X_4 - 2.7187X_2X_3 - 1.1687X_2X_4 \\ & - 1.7687X_3X_4 + 2.0188X_1X_2X_3 + 11.9187X_1X_2X_4 \\ & + 4.2938X_1X_3X_4 - 5.4063X_2X_3X_4 - 6.6438X_1X_2X_3X_4 \end{aligned} \quad (6)$$

4 Conclusions

The dense cell walls are a significant factor controlling the mechanical properties of metallic foams. This has been achieved to a much greater extent in this study due to the non-use of the binders and use of high compaction pressure. However, using high compaction pressure has a constraint of poor compressibility found in most of the available space holder materials. In order to maintain the uniformity of the pore size and shape the space holder material should invariably have some compressibility. This study shows that acrawax could be one such potential material which can resist high compression pressure by changing its lateral dimensions. Controlling the compaction pressure within permissible limits, uniform sized pores with dense cell walls and minimum micro-porosity could be achieved using this space holder material. The lubricating surface of acrawax proved beneficial in achieving better flow of powder particles around acrawax forming better densified cell walls. The mathematical model obtained in this study would be beneficial in obtaining the final porosity and pore sizes in the foam without going for extensive experimentation.

Acknowledgements The first author wishes to thank the Director, CSIR-Advanced Materials and Processes Research Institute, Bhopal, Dr. O.P. Modi and Mr. G.K. Gupta, MCNC group, CSIR-AMPRI, Bhopal for making this work possible.

Funding The funding was provided by Council of Scientific and Industrial Research and National Institute of Technology, Kurushetra.

References

1. N. Dukhan, *Metal Foams: Fundamentals and Applications*, 1st edn, (Destech Publications, Inc., Pennsylvania, USA, 2013)
2. R. Goodall, in *Advances in Powder Metallurgy: Properties, Properties and Applications*, ed. by I Chang, Y Zhao (Woodhead publishing limited, Oxford, 2013), p. 273
3. N. Michailidis, F. Stergioudi, A. Tsouknidas, E. Pavlidou, Mater. Sci. Eng. A **528**, 1662 (2011)
4. R. Surace, L.A.C. De Filippis, A.D. Ludovico, G. Boghetich, Mater. Des. **30**, 1878 (2009)
5. H. Bafti, A. Habibolahzadeh, Mater. Des. **31**, 4122 (2010)
6. M. Alizadeh, M. Mirzaei-Aliabadi, Mater. Des. **35**, 419 (2012)
7. H. Jo, Y.H. Cho, M. Choi, J. Cho, J. Um, Y.E. Sung, H. Choe, Mater. Chem. Phys. **145**, 6 (2014)
8. A. Etiemble, J. Adrien, E. Maire, H. Idrissi, D. Reyter, L. Roue, Mater. Sci. Eng. B **187**, 1 (2014)
9. H.T. Cui, App. Ther. Eng. **39**, 26 (2012)
10. C.N. Ahmed, M. El-Hadek, Adv. Mater. Sci. Eng. (2016) doi:10.1155/2016/9796169
11. F. Xie, X. He, J. Yu, M. Wu, X. He, X. Qu, J Porous Mater. **23**, 783 (2016)
12. Y. Hangai, T. Morita, S. Koyama, O. Kuwazuru, N. Yoshikawa, J Mater. Eng. Per. **25**, 3691 (2016)
13. B. Soni, S. Biswas, J Porous Mater. (2016). doi:10.1007/s10934-016-0233-9
14. A.M. Parvanian, M. Saadatfar, M. Panjepour, A. Kingston, A.P. Shepperd, Mater. Des. **53**, 681 (2014)
15. M. Parvanian, M. Panjepour, Mater. Des. **49**, 834 (2013)
16. B. Ye, D.C. Dunand, Mater. Sci. Eng. A **528**, 691 (2010)
17. N. Jha, D.P. Mondal, J.D. Majumdar, A. Badkul, A.K. Jha, A.K. Khare, Mater. Des. **47**, 810 (2013)
18. J. Jakubowicz, G. Adamek, M. Devidar, J. Porous Mater. **20**, 1137 (2013)
19. A. Mansourighasri, N. Muhamad, A.B. Sulong, J. Mater. Proc. Technol. **212**, 83 (2012)
20. M. Sharma, G.K. Gupta, O.P. Modi, A. B.K Prasad, K. Gupta, Mater. Lett. **65**, 3199 (2011)
21. M. Sharma, G. K. Gupta, O. P. Modi, B. K. Prasad, Powder Metall. **56**, 55 (2013)

22. N. Bekoz, E. Oktay, J. Mater. Process. Technol. **212**, 2109 (2012).
23. I. Mutlu, E. Oktay, J. Porous Mater. **19**, 433 (2012)
24. Z. Esen, S. Bor, Scr. Mater. **56**, 341 (2007)
25. Y.Y. Zhao, T. Fung, L.P. Zhang, F.L. Zhang, Scr. Mater. **52**, 295 (2005)
26. B. Wang, E. Zhang, Int. J. Mech. Sci. **50**, 550 (2008)
27. Y. Mu, G. Yao, L. Liang, H. Luo, G. Zu, Scr. Mater. **63**, 629 (2010)
28. P. Schuler, S.F. Fischer, A. B-Polaczek, C. Fleck, Mater. Sci. Eng. A **587**, 250 (2013)
29. A. Rabiei, L.J. Vendra, Mater. Lett. **63**, 533 (2009)
30. N.Q. Zhao, B. Jiang, X.W. Du, J.J. Li, C.S. Shi, W.X. Zhao, Mater. Lett. **60**, 1665 (2006)
31. M.A. El-Hadek, S. Kaytbay, Int. J. Mech. Mater. Des. **4**, 63 (2008)
32. http://www.fankim.com/media/Acrawax-C_powder.pdf. Accessed 08 Nov 2016
33. http://www.tarakchemicals.com/business-ethylene-bis-stearamide.html. Accessed 08 Nov 2016
34. D.P. Mondal, M. Patel, S. Das, A.K. Jha, H. Jain, G. Gupta, S.B. Arya, Mater. Des. **63**, 89 (2014)
35. D.P. Mondal, M. Patel, H. Jain, A.K. Jha, S. Das, R. Dasgupta, Mater. Sci. Eng. A **625**, 331 (2015)
36. X. Yang, S.J. Guo, B.F. Chen, F. Meng, Y.D. Lian, Powder Technol. **164**, 75 (2006).
37. S.S. Su, I.T.H. Chang, W.C.H. Kuo, Mater. Chem. Phys **139**, 775 (2013)
38. Y.M.Z. Ahmed, M.I. Riad, A.S. Sayed, M.K. Ahlam, M.E.H. Shalabi, Powder Technol. **175**, 48 (2007)
39. P. Langston, A.R. Kennedy, Powder Technol. **268**, 210 (2014)
40. P.C. Angelo, R. Subramanaiam, 1st edn. *Powder Metallurgy: Science, Technology and Applications* (PHI Learning Pvt Ltd, India, 2008)
41. B. Arifvianto, M.A. Leeflang, J. Zhou, Mater. Charact. **121**, 48 (2016)
42. M. Khodaei, M. Meratian, O. Savabi, M. Razavi, Mater. Lett. **171**, 308 (2016)
43. M. H. Shahzeydi, A. M. Parvanian, M. Panjepour, Mater. Charact. **111**, 21 (2016)